Proceedings of the 21st International Conference on Modelling and Applied Simulation (MAS), 025
19th International Multidisciplinary Modeling & Simulation Multiconference

2724-0037 © 2022 The Authors.
doi: 10.46354/i3m.2022.mas.025

Wind turbine pitch and active tower damping control using metaheuristic multi-objective bat optimization

Adrian Gambier[1,*] and Yul Yunazwin Nazaruddin[2]

[1]Fraunhofer IWES, Fraunhofer Institute for Wind Energy Systems, Am Seedeich 45, Bremerhaven, 27572, Germany
[2]Institut Teknologi Bandung, Bandung 40132, Indonesia

[*]Corresponding author. Email address: adrian.gambier@iwes.fraunhofer.de, agambier@ieee.org.

Abstract

Collective pitch control (CPC) is normally combined with an active tower damping control (ATDC) and both control loops are commonly found in the control system of very large wind turbines. Normally, each controller is fine-tuned individually. However, the control loops have a conflict of interest: whereas the CPC keeps the rotational speed constant during overrated wind speed and introduces significant oscillations in the tower subsystem, the ATDC reduces the tower oscillations while detuning the CPC. Thus, the aim of the present contribution is to find an optimal balance where cooperative tuning of both controllers leads to the best possible performance of both controllers with the fewest reciprocal negative effects. In order to achieve the goal, the multi-objective bat algorithm is utilized to obtain all controller parameters. The effectiveness of the methodology is shown by means of a simulation example.

Keywords: Wind turbine; pitch control; tower damping control; multi-objective bat algorithm

1. Introduction

The current state of wind turbine development is dominated by three-bladed, upstream, variable pitch, variable speed machines. They are also growing in size, but with limitations on the amount of material that can be used. This has led to a higher flexibility of both rotor blades and tower, with the direct consequence of large amplitudes of the coupled oscillations. Moreover, during overrated wind speed operation, the rotor speed is maintained constant by pitching all blades simultaneously (collective pitching). This action causes disturbances in the aerodynamic thrust forces, also increasing the tower oscillations.

In order to reduce the oscillations produced by the pitching activities, it is proposed in Bossanyi, (2000) to introduce damping injection into the collective pitch control (CPC) system. The idea of artificial damping injection has its origin in robotics and can already be found in Takegaki and Arimoto, (1981). It is directly correlated to strict passivity (see, e.g., Ortega et al., (1994)). It is shown in Ortega et al., (1994) that damping injection is possible without speed measurement. However, the tower acceleration is normally measured in large wind turbines, and hence, the speed is obtained by integration.

The damping injection in the collective pitch control system in order to actively damp fore-aft tower oscillations (active tower damping control ATDC) has also been studied in Leithead and Domínguez, (2004), Bossanyi, (2003), Wright and Fingersh, (2008) and Murtagh et al., (2008). In the simplest configuration, two control signals from two coupled control loops are added for mutual compensation and act jointly on all pitch actuators.

The current approach consists in adding to the pitch control an additional control loop of the fore-aft tower speed. For example, Shan and Shan, (2012) proposes two PID (Proportional Integral Derivative) controllers. The first controller is used for pitch control and the second one is devoted to the active tower damping. The design is done in two stages. The collective pitch control is adjusted in the first stage, and the tower damping controller is included in the second stage. At each design stage, the controller parameters are tuned by using traditional methods. However, parameter tuning can also be carried out heuristically. This procedure is normally laborious and

the result is not optimal. If the control loops are not strongly coupled, an iterative tuning procedure can be used as proposed in Burton et al., (2011).

Because the aerodynamic torque and the aerodynamic thrust force are closely related, the active tower damping and the pitch control should be conjointly designed. Nevertheless, designing multiple interconnected controllers at the same time is a difficult challenge Brosilow and Joseph, (2002). A solution to this problem is proposed by using multi-objective optimization in Gambier et al., (2006) and applied to wind turbines in Gambier, (2017), Gambier and Nazaruddin, (2018). The optimization is undertaken by using the NBI algorithm (Normal Boundary Intersection Das and Dennis, (1998)) and the MOPSO (Multi-Objective Particle Swarm Optimization Coello and S., (2002)), respectively. Both studies make use of simple dynamic models of the NREL 5 MW reference wind turbine Jonkman et al., (2009), which is derived from a high-resolution model. Additional information about MOO control can be found in Gambier and Badreddin, (2007) and Gambier and Jipp, (2011).

In the comparison presented in Gambier, (2022), it is pointed out the good performance of a simple implementation of Multi-objective Bat algorithm (MOBA Yang, (2011)). Moreover, positive evaluations of bat algorithms are also reported in Gandomi et al., (2013), Li and Zhou, (2014), Rajalakshmi et al., (2021). The algorithm is also efficient for solving nonlinear optimization problems. Thus, there exists a concrete motivation for further studies on the behavior of this algorithm in relation to multi-objective optimal control in general and also control of very large wind turbine in particular.

In this paper, the approach proposed in Gambier et al., (2006) for tuning multiple controllers concurrently is applied to achieve an optimal compromise between both above mentioned control loops (CPC and ATSC). The design approach depends on the application and on the multi-objective optimization approach. Wind turbines are changing with time (e.g., from 5 MW to 20 MW), and many new MOO algorithms have been proposed in recent years (e.g., MOBA). Hence, the contribution of this paper is the control of a modern 20 MW wind turbine (which is not much studied at present) by using the promising MOO Bat algorithm (MOBA Yang, (2011)). In addition, the used model includes more details than those used in previous works, and the reference wind turbine is a modified version of the 20 MW machine proposed in Ashuri et al., (2016).

The paper is organized as follows. In Section II, the control problem is explained in detail, covering several aspects. Designs of the collective pitch control system, active tower damping control system, and a gain scheduling mechanism are presented in Section III. The simultaneous tuning of controllers by using the multi-objective optimization approach, including decision making, is the topic of Section IV. Section V is devoted to describing the reference wind turbine, the parameters and simulation experiments such that the simulation results are presented in Section VI. Finally, the conclusions are drawn in Section VII.

2. Description of the Control Problem

2.1. Operational regions

The operation of an upstream horizontal-axis variable-speed variable-pitch wind turbine is well known (see, for instance, Burton et al., (2011), Manwell et al., (2009), Bianchi et al., (2007), Gambier, (2022)), thus it is discussed briefly in the sequel for completeness.

Depending on the wind speed, the operation of the wind turbine can be separated into four regions. The machine is unable to produce in the first region because the wind speed is less than the design *cut-in* value of the wind speed. When the wind speed exceeds the cut-in value, the machine operation switches to the second region. There the wind speed is sufficient to produce but not enough to reach the rated value. Hence, the control objective is to generate power as much as possible by following the optimal characteristic curve of the generator. The control variable is the electromagnetic torque, which is manipulated by means of power converters.

The operation continues in the second region until the wind speed surpasses the rated value, at which point it moves to the third region. In this region, the control objective is to maintain constant rotational speed (and indirectly, power) by pitching the rotor blades to the feather. Such changes in the pitch angle, on the other hand, cause thrust force disturbances that augment the amplitude of the fore-aft low-damped tower oscillations. As it was previously mentioned, tower oscillations can be attenuated by using damping injection.

The operation in the third region continues until the wind speed goes above the cut-out threshold. In such case, the machine has reached the fourth region and must be shut down for safety reasons.

Finally, the transition between the first and second regions is sometimes called Region I½. The transition between regions two and three is known as Region II½. All regions are described in Figure 1.

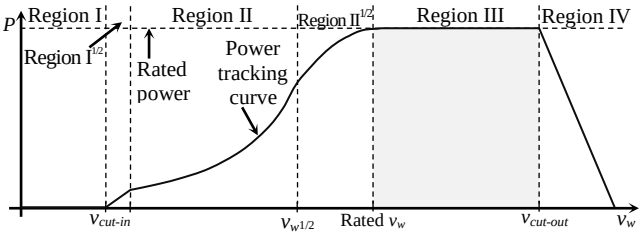

Figure 1. Operational regions of an upstream horizontal-axis variable-speed variable-pitch wind turbine Gambier, (2022)

2.2. Control Loops

The control problem treated in the current work takes place during the operation in Region III. First and most importantly, is the regulatory control to limit the constant rotational speed to the rated value. In second place is the damping of the tower oscillations. Thus, the pitch control system for Region III consists of two control loops,

where the system has one input (the pitch angle) and two outputs (the rotor speed and the tower acceleration).

It should be mentioned that the tower speed is necessary for the damping injection concept. However, the available measured variable is the tower acceleration and therefore an additional integrator is necessary for the control system implementation.

β_0 is the value for the pitch angle, which is set as operating point, since it is a nonlinear system controlled by a linear controller. The value of β_0 depends on the wind speed, i.e., β_0 is the pitch angle necessary to maintain the rotational speed at its rated value for a given wind speed.

Low-pass filters at the blade passing frequency (3P) and notch filters at the free-free drivetrain resonance frequency, which are typically connected in cascade are used to eliminate frequencies, which are present in the measured signals in order to avoid exciting turbine modes and structural resonance frequencies. The control system configuration is presented in Figure 2.

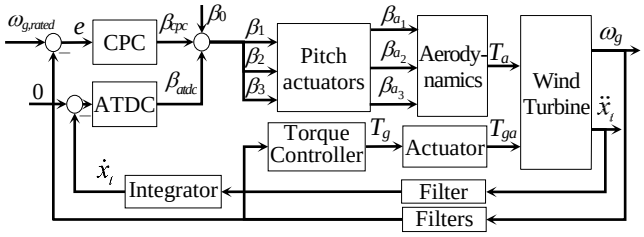

Figure 2. Configuration of the control system topology of a wind turbine

It is worth noting that both control loops share the same input variable, thus they are directly coupled. As a result, both controllers should be jointly parametrized.

On the other hand, the torque controller is essential for the control in the second region, but it is also present in the third one. The simplest control law is optimal torque control (OTC) given by

$$T_g(t) = K_o \omega_g^2(t). \tag{1}$$

The gain K_o is the optimal value obtained for the stationary power maximization, ω_g is the generator speed and T_g the generator torque.

3. Control approach

The control approach includes two control loops acting on the pitch angle. For the most important control loop, a PI (proportional integral) control law is used. The second control loop is based on a PD (proportional derivative) controller. Linear controllers working with a nonlinear system must include adaptation and the integrator needs an anti-windup mechanism.

3.1. Collective Pitch Control

The PI control law defined in frequency domain by

$$G_{PI}(s) = K_p + \frac{K_i}{s} = \frac{K_i + K_p\, s}{s}, \tag{2}$$

where K_p and K_i are the controller gains. The linear controller is tuned at a specific operating point and, therefore, it will work inappropriately if the operating point changes. Thus, the controller parameters have to be retuned. This can be obtained by using the gain-scheduling strategy, which can be seen as a simple adaptive procedure. Gain-scheduling adaptation can be accomplished in a number of ways. The approach used here follows Gambier, (2022) and relies on pole placement because it ensures stability at all operating points, which are determined by wind speeds.

Assuming a first order system with transfer function

$$G(s) = \frac{B(s)}{A(s)} = \frac{b_0}{s + a_1}, \tag{3}$$

the design procedure is based on the pole placement approach for the closed loop control system. Thus, the characteristic equation of the closed control system based on the PI controller is given by

$$s^2 + (a_1 + b_0 K_p)s + b_0 K_i = 0. \tag{4}$$

The characteristic equation proposed for the closed loop system is defined by

$$\wp(s) = s^2 + 2\zeta\omega_n s + \omega_n^2 = 0, \tag{5}$$

where parameters ω_n and ζ are natural frequency and the damping ratio, respectively, which are selected by design. Comparing (4) und (5), the coefficients are

$$a_1 + b_0 K_p = 2\zeta\omega_n \text{ and } b_0 K_i = \omega_n^2, \tag{6}$$

and consequently

$$K_p = (2\zeta\omega_n - a_1)/b_0 \text{ and } K_i = \omega_n^2 / b_0. \tag{7}$$

The rotating subsystem is simplified to be represented by

$$J_e\, \Delta\dot{\omega}_r + B_e\, \Delta\omega_r = T_a - n_x T_g, \tag{8}$$

where J_e and B_e are the equivalent mass moment of inertia and the equivalent damping coefficient, respectively. T_a is the aerodynamic torque acting on the drive train and T_g is the generator reaction. n_x is the gearbox ratio.

In the third region under perfect rotor speed regulation, it is assumed $\omega_r = \omega_{r,rated}$ and $\omega_g = n_x \omega_r$. Hence, the aerodynamic torque is described in terms of power as

$$T_a = \frac{P(\beta, \omega_{r,rated})}{\omega_{r,rated}}. \tag{9}$$

Expressing K_o also in terms of power, i.e., $K_o = P_{rated} / \omega_g^3$, the control law for the generator torque becomes

$$T_g = K_{opt}\omega_g^2 = P_{rated} / \omega_g = P_{rated} / (n_x\, \omega_r). \tag{10}$$

Introducing (9) and (10) into the right side of (8), it follows

$$T_a - n_x T_g = \frac{P(\beta, \omega_{r,rated})}{\omega_{r,rated}} - n_x \frac{P_{rated}}{n_x \omega_r}. \quad (11)$$

and linearizing

$$T_a - n_x T_g = \frac{1}{\omega_{r,rated}} \frac{\partial P}{\partial \beta}\bigg|_{\beta_0} \Delta\beta + \frac{P_{rated}}{n_x \omega_{r,rated}^2} \Delta\omega_r + \cdots. \quad (12)$$

Finally, (8) becomes

$$J_e \Delta\dot{\omega}_r + B_e \Delta\omega_r == \frac{1}{\omega_{r,rated}} \frac{\partial P}{\partial \beta}\bigg|_{\beta_0} \Delta\beta + \frac{P_{rated}}{n_x \omega_{r,rated}^2} \Delta\omega_r. \quad (13)$$

Hence, the transfer function in terms of ω_g is obtained after Laplace-transformation as

$$G(s) = \frac{\frac{n_x^2}{J_e \omega_{g,rated}} \frac{\partial P}{\partial \beta}\Big|_{\beta_0}}{s + [B_e - n_x P_{rated} / \omega_{g,rated}^2] / J_e}. \quad (14)$$

Comparing (3) with (14), it follows

$$b_0 = \frac{n_x^2}{J_e \omega_{g,rated}} \frac{\partial P}{\partial \beta}\bigg|_{\beta_0} \text{ and } a_1 = \frac{B_e - n_x P_{rated} / (\omega_{g,rated}^2)}{J_e}. \quad (15)$$

The adaption law (7) is then used with (15) for given design parameters ω_n and ζ in order to obtain the controller when operating point changes. The partial derivative $\partial P/\partial\beta$, which is known as sensitivity function, at the operating point is utilized as a scheduling parameter.

It is important to mention that (7) provides parameters, which are not necessarily optimal. They are also independent of the other control loop and therefore they should be used as start values for the optimization process.

3.2. Active Tower Damping Control

A PD controller has the property of enhancing the damping of a closed loop control system, Visioli, (2006). Therefore, the aim here is to design a control loop based on PD controller that connects the fore-aft tower speed and the pitch angle. In the time domain, an ideal PD controller can be formulated by

$$\Delta\beta_{atdc}(t) = K_{p,atdc} e(t) + K_{d,atdc} \dot{e}(t). \quad (16)$$

The fore-aft tower top displacement is denoted by $x_t(t)$, and the reference for the controller is $x_{to}(t)$. Assuming that the set point coincides with the tower rest position, where the coordinate axis is specified, then the reference can be defined as equal to zero. The control error is denoted by $e(t) = x_{to}(t) - x_t(t)$ and its derivative as $\dot{e}(t) = \dot{x}_{to}(t) - \dot{x}_t(t)$. Hence, the control law can be rewritten as

$$\Delta\beta_{atdc}(t) = -[K_{p,atdc} \Delta x_t(t) + K_{d,atdc} \Delta\dot{x}_t(t)]. \quad (17)$$

The fore-aft tower dynamics is described by the second-order differential equation

$$m_t \ddot{x}_t + D_t \dot{x}_t + K_t x_t = F_t(\beta) + (1.5/h_t) T_t. \quad (18)$$

where K_t, D_t, m_t and h_t represent the tower modal stiffness, modal damping, modal mass and tower height, respectively. T_t and F_t are the aerodynamic tilt moment and the thrust force, which depends on the pitch angle β.

Assuming that the tower behaves as a prismatic beam, which is loaded at one extreme, the factor (1.5/ht) represents the ratio between the bending and rotation of the tower top. The linear equation

$$m_t \Delta\ddot{x}_t + D_t \Delta\dot{x}_t + K_t \Delta x_t = [(\partial F_t / \partial\beta)_{\beta_0} + (1.5/h_t)(\partial T_t / \partial\beta)_{\beta_0}] \Delta\beta. \quad (19)$$

is obtained by linearizing (18) around β_0. The difference variable Δx_t defined as $\Delta x_t = x_t - x_{to}$ with x_{to} as the operating point. Inserting the control law (17) into the model (19), one obtains

$$m_t \Delta\ddot{x}_t + [D_t + [(\partial F_t / \partial\beta)_{\beta_0} + (1.5/h_t)(\partial T_t / \partial\beta)_{\beta_0}] K_{d,atdc}] \Delta\dot{x}_t + [K_t + [(\partial F_t / \partial\beta)_{\beta_0} + (1.5/h_t)(\partial T_t / \partial\beta)_{\beta_0}] K_{p,atdc}] \Delta x_t = 0. \quad (20)$$

Comparing (19) and (20), it follows that the closed control system increases the damping and the stiffness coefficients according to the terms

$$[(\partial F_t / \partial\beta)_{\beta_0} + (1.5/h_t)(\partial T_t / \partial\beta)_{\beta_0}] K_{d,atdc} \text{ and} \quad (21)$$

$$[(\partial F_t / \partial\beta)_{\beta_0} + (1.5/h_t)(\partial T_t / \partial\beta)_{\beta_0}] K_{p,atdc}, \quad (22)$$

respectively. The proportional term of the controller leads to an increment in the stiffness coefficient and, therefore, in the first natural frequency. To avoid this change in frequency, the proportional gain $K_{p,atdc}$ is set equal to zero. The derivative gain $K_{d,atdc}$ can be computed for a desired damping coefficient as D_{tf}, by equating this value of D_{tf} to the damping coefficient of (20), i.e.,

$$D_t + [(\partial F_t / \partial\beta)_{\beta_0} + (1.5/h_t)(\partial T_t / \partial\beta)_{\beta_0}] K_{d,atdc} = D_{tf}. \quad (23)$$

Hence, the derivative gain is obtained as

$$K_{d,atdc} = \frac{D_{tf} - D_t}{(\partial F_t / \partial\beta)_{\beta_0} + (1.5/h_t)(\partial T_t / \partial\beta)_{\beta_0}}. \quad (24)$$

The dependence of T_t with respect to β is in general not relevant and the factor $(1.5/h_t) << 1$ such that the second term in the denominator can be omitted. On the other hand, the desired damping coefficient D_{tf}, can be chosen as factor of the physical damping D_t i.e., $D_{tf} = \gamma_t D_t$ with $\gamma_t > 1$. For a constant set point, its derivative is $\dot{x}_{to}(t) = 0$ and the control law (17) becomes

$$\Delta\beta_{atdc}(t) = -\frac{(\gamma_t - 1) D_t}{(\partial F_t / \partial\beta)_{\beta_0}} \dot{x}_t(t). \quad (25)$$

The value for the sensibility function $\partial F_t/\partial\beta$ at the current pitch angle is a scheduling parameter to correct the gain when the wind speed changes, providing a gain-sched-

uling adaption for the active tower damping control.

It should be remarked that $\gamma_t > 1$ is selected for a "desired" damping of the tower. However, this way of finding the controller gain is not always acceptable because the gain is not really a free parameter. On the one hand, the desired value for the damping must be physically acceptable and, on the other hand, all controllers are subjects to the pitch actuator constraints. Hence, (25) can provide a start value for the gain, but the fine-tuning including actuator constraints requires a more complex procedure that includes optimization.

4. Tuning the Control System

4.1. Description of the Method

The used methodology for the tuning of a multi-loop control system with several controllers follows the ideas presented in Gambier, (2017), Gambier and Nazaruddin, (2018), Gambier et al., (2006). It consists in considering the controllers of a coupled multi-loop control system as participants in a nonzero-sum cooperative dynamic game Haurie, (2001), Petrosjan, (2005), Schmitendorf, (1972). An objective function (payoff) is assigned to each participant, resulting in the vector-valued function

$$\mathbf{J} = [J_1 \quad J_2 \quad \cdots \quad J_m]^{\mathrm{T}}. \tag{26}$$

for the game (control system). The total number of controllers (players in the game) is given by m, and each player has an individual cost function J_i. Furthermore, the game is dynamic due to the presence of a dynamic feedback system, i.e., a cooperative differential game.

Multi-objective optimization (MOO) can be used to solve the game, and Pareto methods have the advantage that they process all objective functions J_i separately but handles the contradictory objectives concurrently, Bernard, (2005). The optimum in the sense of Pareto is a set of non-dominated solutions (optimal Pareto set, Giesy, (1978)). Non-dominated solutions are ones in which improving any objective does not degrade the others. Finally, the optimal parameters for the controllers are obtained by using a decision maker, which takes one solution from the Pareto optimal set.

4.2. Multi-objective Bat Algorithm (MOBA)

The multi-objective bat algorithm (MOBA) is derived from the multi-objective particle swarm optimization (MOPSO), which in turn is a subclass included in the metaheuristic-programming-based methods.

Particle swarm intelligence is a stochastic optimization procedure based on a population of particles similar to evolutionary algorithms. However, all particles survive the whole process until the last generation, while evolving individuals can also disappear during the process. Particles search the space of variables by utilizing knowledge from previous generations and migrating at a specific computed speed in the direction of the global best particle. Several algorithms have been developed based on this paradigm, with the main goal of imitating the behavior of various swarms or colonies of creatures such as ants, bees and bats.

The bat algorithm (BA) has been proposed first in Yang, (2010) and extended to the multi-objective case in Yang, (2011). It is based on an idealization of the echolocation sense of microbats. Assumptions to generate the algorithm can be formulated as follows:

1. In order to detect distance, all bats utilize echolocation. In some manner, they can distinguish food from background obstacles.
2. Bats look for prey by flying at an arbitrary velocity v_i at position x_i with a frequency f_{min}, variable wavelength λ and loudness A_0. Depending on the closeness to their target, they modify automatically the frequency (or wavelength) of their radiated pulses as well as the rate of pulse emission $r \in [0, 1]$.
3. In general, the loudness can change in many forms. However, it is adopted here that the loudness varies from a large positive number A_0 to a minimum constant value A_{min}.
4. In order to reduce the computational burden in multi-dimensional cases, the time delay and three-dimensional topography are not calculated via ray tracing.
5. It is also assumed that the frequency f in a range $[f_{min}, f_{max}]$ corresponds to the range of wavelengths $[\lambda_{min}, \lambda_{max}]$.

The motion of the i^{th} bat is modeled by

$$\mathbf{x}_i(k+1) = \mathbf{x}_i(k) + \mathbf{v}_i(k), \tag{27}$$

$$\mathbf{v}_i(k+1) = \mu\,\mathbf{v}_i(k) + f_i[\mathbf{x}_i(k) - \mathbf{x}^*], \text{ and} \tag{28}$$

$$f_i = f_{min} + \boldsymbol{\rho}(f_{max} - f_{min}), \tag{29}$$

where $k = 0, 1, \Lambda$ is the iteration number, $\mathbf{x}_i(k)$ and $\mathbf{v}_i(k)$ are the position and velocity of bat i at iteration k. $\mathbf{x}^*$ denotes the current global best solution. It is obtained by comparison between the solutions of all bats at iteration k. The speed increment is given by the product $\lambda_i f_i$, where f_i is the frequency and λ_i is the wavelengths. $\boldsymbol{\rho} \in [0, 1]$ is a random vector, which is obtained from a uniform distribution.

The constant μ in (28) is known as the inertia weight factor. In the classic approach of Yang, (2010), μ is equal to one. However, there are now constant and random, linear and nonlinear, time-variant and adaptive approaches (see Nickabadi et al., (2011) for a review of techniques).

On the other hand, bats randomly walk around the current best solution, and the position is locally updated by

$$\mathbf{x}_{new}(k) = \mathbf{x}_{current}(k) + \sigma\hat{\boldsymbol{\theta}}(k)\sum_{i=1}^{n} A_i(k)/n, \tag{30}$$

where $\int$ is a random number with Gaussian normal distribution N(0, 1) and σ is a scaling factor (equal to one in the classic case). The loudness A_i normally reduces after a bat has found its prey, and contrarily the rate of pulse

emission r_i increases. The laws for updating these parameters are given by

$$A_i(k+1) = \alpha A_i(k), \quad (31)$$

$$r_i(k) = r_i(0)(1-e^{-\gamma k}), \quad (32)$$

in which $0 < \alpha < 1$ and $\gamma > 0$ are constants.

In the multi-objective case, the problem is solved by using a weighted sum, where the weights are obtained by random generation. It is important that such generation is carried out with enough diversity in order to guarantee a correct estimation of the Pareto front. Finally, a non-dominated sorting process takes place, followed by ranking and calculation of crowding distances. A pseudo code for the MOBA is summarized in Algorithm 1.

Algorithm 1: Pseudo code for MOBA from Yang, (2011)

Objective functions $J_1(\mathbf{x}), ..., J_m(\mathbf{x})$, $\mathbf{x} = [x_1, ..., x_d]^T$
Initialize the bat population $\mathbf{x}_i$ and $\mathbf{v}_i$ ($i = 1, 2, ..., n$)
for $j = 1$ to n_p (number pf points on Pareto fronts)
    Create m weights $w_p \geq 0$ *satisfying* $\sum_p^m w_p = 1$
    Build the weighted sum objective $J_{ws} = \sum_p^m w_p J_p$
    while $t < t_{Max}$ (given by number of iterations)
        Compute new solutions and update by (27) - (29)
        if a random number between [0,1] > r_i
            do a random walk around the selected best solution
        end if
        Produce a new solution by flying randomly
        if (a random number between [0,1]) < A_i) and ($f(\mathbf{x}_i) < f(\mathbf{x}^*)$)
            accept the new solutions,
            increase r_i and *reduce* A_i *by using* (30) – (31)
        end if
        Reorder the bats and find the current best $\mathbf{x}^*$
    end while
    Save $\mathbf{x}^*$ *as a non-dominated solution*
end for
Start graphic representation of the Pareto front

4.3. Decision making

The compromise solution (CS), i.e., the solution with the shortest distance from the Pareto front to the utopia point, is chosen as the final option by the majority of decision makers.

Another option is to use bargaining games Thomson, (1994), which provide a useful way to choose a single point from the Pareto front. The most typical solutions to bargaining games are illustrated in Figure 3.

The Nash solution (NS) is a point in the Pareto set that produces the largest rectangle (c, B, NS, A). The intersection point between the Pareto front and the straight line connecting the threat and utopia points is known as the Kalai-Smorodinsky solution (KS). The last choice is the egalitarian solution (ES), which is given as a result of the intersection between the Pareto front and a 45-degree straight line through the threat point.

5. Numerical Study

5.1. Simulation Model

In order to study the behavior of the MOBA, a reference wind turbine of 20 MW is used. This is the reference

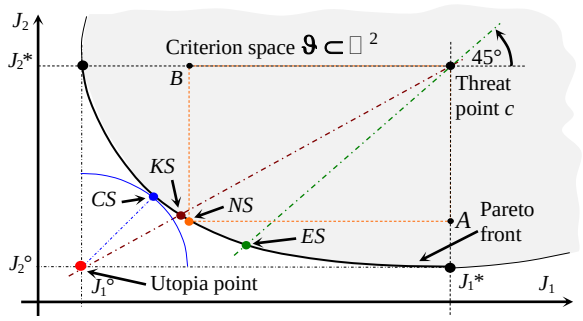

Figure 3. Different solutions for a bargaining game as a decision maker

turbine presented in Ashuri et al., (2016) and studied from the control point of view in Gambier and Meng, (2019). However, the reference wind turbine has been modified in order to introduce drivetrain losses with an efficiency of 97.8%. In order to maintain the rated power and the rated generator speed, the operating point has been lightly modified as shown in Table 1.

Table 1. Properties of the 20 MW reference wind turbine.

Parameter	Name	Old Values	New Values	Units
Rated power	P_{rated}	20.00	20.00	MW
Rated generator speed	$\omega_{g,rated}$	1173.7	1173.74	rpm
Rated wind speed	$v_{w,rated}$	10.70	10.78	m/s
Rated rotor speed	$\omega_{r,rated}$	7.1567	7.1569	rpm
Rated generator torque	$T_{g,rated}$	0.1725	0.1718	MN m
Rated aerodynamic torque	$T_{a,rated}$		28.887	MN m
Generator efficiency	η_g	94.4	94.61	%
Drivetrain efficiency	η_{dt}	100	97.9	%

The essential parameters of the reference wind turbine, which are necessary in order to solve (15) and (24), are presented in Table 2.

Table 2. Essential parameters of the 20 MW reference wind turbine

Parameter	Name	New Values	Units
Equivalent mass moment of inertia	J_e	3.1146×10^9	kg m^2
Equivalent shaft damping coefficient	B_e	4.97×10^7	Nm/(rad/s)
Gearbox ratio	n_x	164	---
Tower damping coefficient	D_t	7.7729×10^9	
Tower height (hub height)	h_t	160.2	m

The data for the needed partial derivatives is presented in Figure 4.

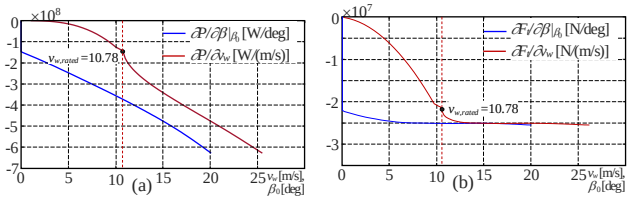

Figure 4. Derivatives of power (a) and thrust force (b) with respect to pitch angle and wind speed.

5.2. Optimization problem

Controller parameters for the CPC can be computed by using (7) and (15), where the design parameters ω_n and ζ are needed. According to Hansen et al., (2005), these

parameters can be chosen as ω_n = 0.6 rad/s and $\zeta \cong 0.6 - 0.7$. For (25), γ_t is chosen as 1.1, i.e., for an increase of 10% in the damping coefficient.

Combining the parameters of Table 2 with the data of Figure 4, a sequence of controller parameters for the pitch angles is obtained. By using curve fitting, equations for the controller parameters in dependence of the pitch angle are obtained as

$$K_p = -0.27 e^{-0.2627\beta} - 0.4883 e^{-0.05043\beta}, \quad (33)$$

$$K_i = -0.118 e^{-0.2627\beta} - 0.2123 e^{-0.05043\beta}, \text{ and} \quad (34)$$

$$K_{d,atdc} = 0.02184 - 0.8342 0.27\beta + 10.27\beta^2 - 352.3\beta^3. \quad (35)$$

However, these values depend on the system dynamics and could be inadequate for a particular case. On the other hand, the parameters can be used as start values for the optimization process. Hence, the parameters to be optimized are K_p, K_i and $K_{d,atdc}$, which leads to a parameter vector defined by

$$\boldsymbol{\alpha} = [K_p \quad K_i \quad K_a \quad K_{d,atdc}]^T, \quad (36)$$

$1/K_a$ is the tracking-time constant for the PI anti-wind-up mechanism. The vector objective is constructed as

$$\mathbf{J} = [J_{cpc} \quad J_{atdc}]^T, \quad (37)$$

where the performance indices time-weighted square error (ITSE)

$$J_{cpc} = \int_0^\infty t\,(\omega_{g,rated}(t) - \omega_g(t))^2\,dt, \text{ and} \quad (38)$$

$$J_{atdc} = \int_0^\infty t\,[x_t(t) - x_t(t \to \infty)]^2 dt \quad (39)$$

are used for the CPC and ATDC, respectively.

It is also necessary to define the pitch actuator constraints to include them in the optimization process. The rated generator speed $\omega_{g,rated}$ is achieved at a value of $\beta = \beta_0$ for a specific wind speed. Moreover, the collective pitch controller and the active tower-damping controller have the contributions β_{cpc} and β_{atdc} to the final pitch angle, which can be represented by

$$\beta = \beta_0 + \beta_{cpc} + \beta_{atdc}, \quad (40)$$

On the other hand, the angle traveled by the actuators as well as the speed of their displacement are limited, namely,

$$\beta_{\min} \le \beta \le \beta_{\max} \text{ and } \dot{\beta}_{\min} \le \dot{\beta} \le \dot{\beta}_{\max}. \quad (41)$$

The CPC is the main control loop and therefore, it is accepted that the CPC is able to travel the whole pitch actuator range taking values according to

$$\beta_{\min} - \beta_0 \le \beta_{cpc} \le \beta_{\max} - \beta_0 \text{ and } \dot{\beta}_{\min} \le \dot{\beta}_{cpc} \le \dot{\beta}_{\max}. \quad (42)$$

Finally, the available spans for β_{atdc} and $\dot{\beta}_{atdc}$ are

$$\beta_{\min} - \beta_0 - \beta_{cpc} \le \beta_{atdc} \le \beta_{\max} - \beta_0 - \beta_{cpc} \text{ and} \quad (43)$$

$$\dot{\beta}_{\min} - \dot{\beta}_{cpc} \le \dot{\beta}_{atdc} \le \dot{\beta}_{\max} - \dot{\beta}_{cpc}. \quad (44)$$

Pitch actuator values for the third region are, e.g., β_{min} = -2 deg, β_{max} = 22 deg, $\dot{\beta}_{min}$ = –8 deg/s and $\dot{\beta}_{max}$ = 8 deg/s.

5.3. Optimization procedure and results

The MOBA requires several evaluations of the objective functions at every iteration. There are two methods to do this (see, for instance, Gambier, (2022) for details): model-based and simulation-based computing. In the present work, the simulation-based method is used, in which the objective functions are obtained numerically as part of the simulation. The benefit of this approach is that almost all types of objective functions can be computed. The disadvantage is that simulations must be ended at a finite point in time, and consequently, steady-state values are obtained by approximation after a long simulation time. Therefore, time-averaged objective functions are applied. The simulation-based approach is schematized in Figure 5.

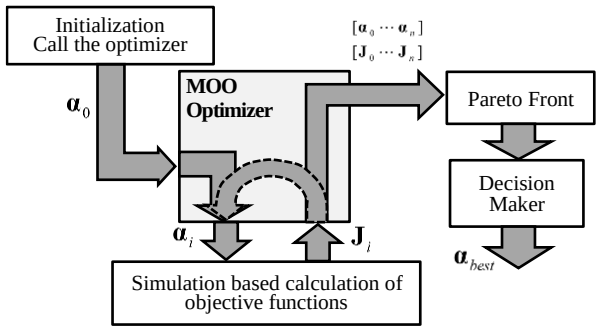

Figure 5. Schematic description of a simulation-based optimization process

Figure **6** shows the obtained Pareto front for the effective wind speed of 11 m/s, where three points are obtained as results of the decision making (CS, KS and NS).

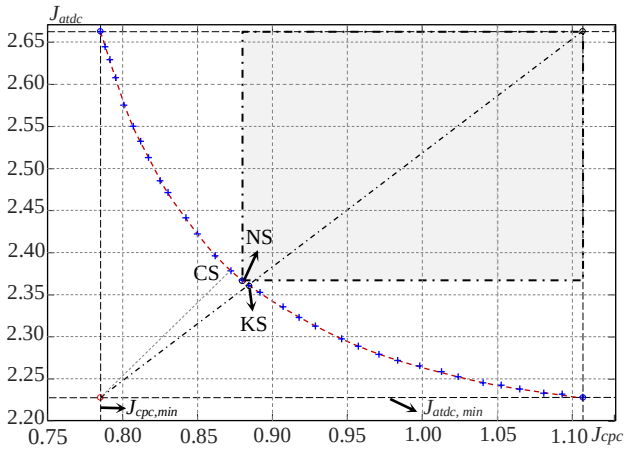

Figure 6. Pareto front for v_w = 11 m/s (J_{cpc} vs. J_{atdc})

The controller parameters are summarized in Table 3. The table also shows the values of the objective functions obtained from the simulation.

Table 3. Cost values and optimized parameters for v_w = 11 m/s

	Eqs. (7), (15) & (25)	CS	NS	KS
J^o_{cpc}	1.528	0.8751	0.8843	0.8911
J^o_{atdc}	12.48	2.3821	2.3703	2.3614
K_p	-0.6248	-1.222	-0.117	-2.52951
K_i	-0.2730	-2.923	-0.1543	-0.3232
K_a	-11.5493	-18.6030	-5.7783	-1.2500
$K_{d,atdc}$	-0.337×10^3	-2.0141×10^4	-1.2126×10^4	-1.4401×10^4

5.4. Simulation Results

The simulations are carried out assuming a stochastic wind profile with a wind speed between 11 and 20 m/s with a piecewise mean value and turbulence of 7%.

Simulation results are presented in Figure 7 for the parameters provided by the KS solution. It is possible to see that the parameters computed by the equations (7), (15) and (25) are not optimal and can be improved by optimization. The reason for this improvement margin is the fact that the models used for the derivation of the equations are very simple. The model parameters also have a certain uncertainty, while the BAT algorithm exploits the high-resolution model, which is used for the simulation.

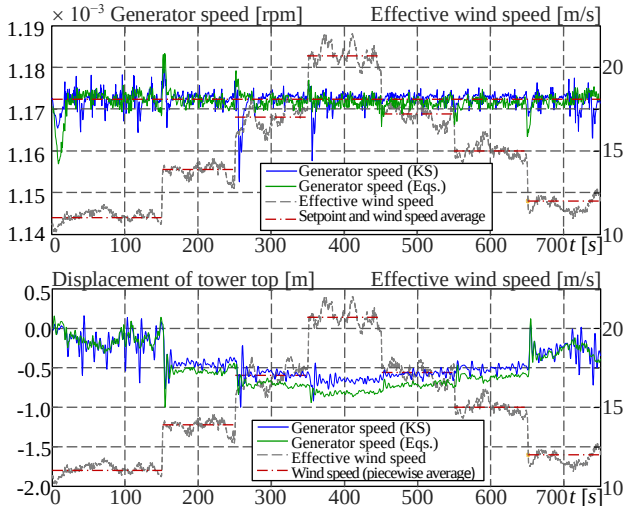

Figure 7. Simulation results for the numerical study.

6. Conclusions

The capacity of the MOBA to tune a multi-loop control system for the control of a very large wind turbine in the overrated wind speed region is studied in this work. The gain scheduling mechanism for the adaption as well as the damping injection approach for the active tower damping control are also derived.

MOBA provides a fast finding of the Pareto front and the decision maker provides the controller parameters for an optimal control performance as a compromise between power production and tower damped oscillation. The simulation results confirm the satisfactory control performance in a numerical way. The next steps in the development will be the inclusion of an individual pitch control (IPC) loop as well as a rotor blade damping control loop.

Funding

This work has been financed by the Federal Ministry of Economic Affairs and Climate Action (BMWK).

References

Ashuri, T., Martins, J. R. R. A., Zaaijer, M. B., van Kuik, G. A. M. and van Bussel, G. J. W. (2016). Aeroservoelastic design definition of a 20 MW common research wind turbine model. *Wind Energy*, 19: 2071 – 2087.

Bernard, T. (2005). Multicriteria optimization of a chemical process with many constraints (in german). Proceedings of the *GMA-Kongress - VDI-Berichte 1883*, Baden-Baden, 393–399, 2005.

Bianchi, F. D., de Battista, H. and Mantz, R. J. (2007). *Wind Turbine Control Systems*, Springer Nature, London, UK.

Bossanyi, E. A. (2000). The design of closed loop controllers for wind turbines. *Wind Energy*, 3: 149 – 163.

Bossanyi, E. A. (2003). Wind turbine control for load reduction. *Wind Energy*, 6: 229 – 244.

Brosilow, C. and Joseph, B. (2002). *Techniques of Model-Based Control*, 1st edn, Prentice Hall, Upper Saddle River, USA.

Burton, T., Jenkins, N., Sharpe, D. and Bossanyi, E. (2011). *Wind Energy Handbook*, 2nd edn, John Wiley & Sons, Chichester, UK.

Coello, C. A. and S., L. M. (2002). MOPSO: a proposal for multiple objective particle swarm optimization. Proceedings of the *2002 Congress on the Evolutionary Computation*, Honolulu, USA, 1051-1056, 2002.

Das, I. and Dennis, J. E. (1998). Normal-Boundary Intersection: A new method for generating the Pareto surface in nonlinear multicriteria optimization problems. *SIAM Journal on Optimization*, 8: 631-657.

Gambier, A. (2008). MPC and PID control based on multi-objective optimization. Proceedings of the *2008 American Control Conference*, Seattle, 2886-2891, 2008.

Gambier, A. (2017). Simultaneous design of pitch control and active tower damping of a wind turbine by using multi-objective optimization. Proceedings of the *1st IEEE Conference on Control Technology and Applications*, Kohala Coast, USA, 1679 – 1684, 27–30 August 2017.

Gambier, A. (2022). *Control of Large Wind Energy Systems*, Springer Nature, Basel, Switzerland.

Gambier, A. (2022). Multiobjective optimal control of wind turbines: A survey on methods and recommendations for the implementation. *Energies*, 15: 567.

Gambier, A. and Badreddin, E. (2007). Multi-objective optimal control: An overview. Proceedings of the *IEEE Conference on Control Applications*, Singapore, 170-175, 2007.

Gambier, A. and Jipp, M. (2011). Multi-objective optimal control: An introduction. Proceedings of the *Asian Control Conference*, Kaohsiung, Taiwan, 1084 – 1089, 15–18 May 2011.

Gambier, A. and Meng, F. (2019). Control system design for

a 20 MW reference wind turbine. Proceedings of the *12th Asian Control Conference*, Hong Kong, 258 – 263, 19–21 August 2019.

Gambier, A. and Nazaruddin, Y. (2018). Collective pitch control with active tower damping of a wind turbine by using a nonlinear PID approach. *IFAC–PaperOnline*, 51: 238 – 243.

Gambier, A., Wellenreuther, A. and Badreddin, E. (2006). A new approach to design multi-loop control systems with multiple controllers. Proceedings of the *45th IEEE Conference on Decision and Control*, San Diego, USA, 1828 – 1833, 13–15 December 2006.

Gandomi, A. H., Yang, X.-S., Alavi, A. H. and Talatahari, S. (2013). Bat algorithm for constrained optimization tasks. *Neural Computing and Applications*, 22: 1239 – 1255.

Giesy, D. (1978). Calculation of Pareto-optimal solutions to multiple-objective problems using threshold-of-acceptability constraints. *IEEE Transactions on Automatic Control*, 23: 1114–1115.

Hansen, M. H., Hansen, A., Larsen, T. J., Øye, S., Sørensen, P. and Fuglsang, P. (2005). Control design for a pitch-regulated, variable speed wind turbine, Technical report, Risø National Laboratory, Roskilde, Denmark.

Jonkman, J., Butterfield, S., Musial, W. and Scot, G. (2009). Definition of a 5-MW Reference Wind Turbine for Offshore System Development, NREL/TP-500-38060, NREL, Golden, Colorado.

Leithead, W. E. and Domínguez, S. (2004). Analysis of tower/blade interaction in the cancellation of the tower fore-aft mode via control. Proceedings of the *European Wind Energy Conference*, London, UK, 1 – 10, 22 – 25 November 2004.

Liu, G. P., Yang, J. B. and Whidborne, J. F. (2003). *Multiobjective Optimisation and Control*, Research Studies Press Ltd., Exeter.

Li, L. and Zhou, Y. (2014). A novel complex-valued bat algorithm. *Neural Computing and Applications*, 25: 1369 – 1381.

Manwell, J., McGowan, J. and Rogers, A. (2009). *Wind energy explained: theory, design, and application*, John Wiley & Sons, Chichester, UK.

Murtagh, P. J., Ghosh, A., Basu, B. and Broderick, B. M. (2008). Passive control of wind turbine vibrations including blade/tower interaction and rotationally sampled turbulence. *Wind Energy*, 11: 305 – 317.

Nickabadi, A., Ebadzadeh, M. M. and Safabakhsh, R. (2011). A novel particle swarm optimization algorithm with adaptive inertia weight. *Applied Soft Computing*, 11: 3658 – 3670.

Ortega, R., Loria, A., Kelly, R. and Praly, L. (1994). On passivity-based output feedback global stabilization of Euler-Lagrange systems. Proceedings of the *33rd IEEE Conference on Decision and Control*, Lake Buena Vista, 381 – 386, 14–16 December 1994.

Rajalakshmi, M., Chandramohan, S., Kannadasan, R., Alsharif, M. H., Kim, M.-K. and Nebhen, J. (2021). Design and validation of BAT algorithm-based photovoltaic system using simplified high gain quasi boost inverter. *Energies*, 14: 1086.

Schmitendorf, W. E. (1972). Cooperative games and vector-valued criteria problems. Proceedings of the *IEEE Conference on Decision and Control*, vol. 18, New Orleans, USA, 340 – 344, 13–15 December 1972.

Shan, W. and Shan, M. (2012). Gain scheduling pitch control design for active tower damping and 3P harmonic reduction, Copenhagen, 2012.

Takegaki, M. and Arimoto, S. (1981). A new feedback method for dynamic control of manipulators. *Journal of Dynamic Systems, Measurement and Control*, 103: 119 – 125.

Visioli, A. (2006). *Practical PID Control*, Springer, London, UK.

Wright, A. D. and Fingersh, L. J. (2008). Advanced control design for wind turbines, Technical Report, National Renewable Energy Laboratory (NREL), NREL/TP-500-42437, Golden, USA.

Yang, X.-S. (2011). Bat algorithm for multi-objective optimisation. *International Journal Bio-Inspired Computation*, 3: 267-274.